Macromolecules

Volume 42, Number 3 February 10, 2009

Communications to the Editor

Spontaneous Formation of Nanoscale Polymer Spheres, Capsules, or Rods by Evaporation of Polymer Solutions in Cylindrical Alumina Nanopores

Xunda Feng and Zhaoxia Jin*

Department of Chemistry, Renmin University of China, Beijing 100872, People's Republic of China

Received October 30, 2008
Revised Manuscript Received December 29, 2008

ABSTRACT: In this study, we report for the first time the fabrication of polymer nanospheres, nanocapsules, and hemispherically capped nanorods simply through the wetting of anodic aluminum oxide (AAO) membranes with polymer solutions. For the wetting with polystyrene solutions, we have demonstrated that the formation of nanorods is dependent upon the solvents used (e.g., tetrahydrofuran and methyl ethyl ketone) which have strongly adsorbent nature toward alumina surfaces, displaying no correlation to molecular weight. More importantly, we have shown that there is a coarsening process from spheres to capsules to rods in AAO cylindrical nanopores during solvent evaporation. The coarsening process could serve as the formation mechanism for nanorods which have the similar diameter as the AAO nanopores. Our observation also provides a facile approach for fabricating polymer nanospheres and nanocapsules that can be directed by cylindrical nanopores into ordered arrays.

Porous anodic aluminum oxide (AAO) membranes have been widely used as templates for fabricating one-dimensional (1D) polymer nanostructures.[1−12] Particularly, the wetting of AAO membranes with polymer melts or solutions has been previously proven to be a simple, versatile approach.[3−12] Although much progress has been made in the fabrication and characterization of 1D polymer nanostructures via template wetting, relatively few reports have concentrated on the underlying physical chemistry of the wetting behavior involved in AAO cylindrical nanopores, which is crucial for the controllable formation of nanostructures. For wetting AAO membranes with polymer melts, Russell et al. have demonstrated that two distinct mechanisms, i.e., partial wetting (capillary force) and complete wetting (precursor film), control the nanorod and nanotube formation respectively.[10] The transition from partial to complete wetting can be achieved by increasing annealing temperature. With respect to the wetting with polymer solutions, Wendorff et al. have recently reported that nanotubes should be obtained from the wetting with high molecular weight polymers, whereas intermediate and low molecular weight polymers favor the formation of void-containing nanorods and solid nanorods respectively.[11] However, it has been unknown so far what mechanisms dominate the morphologies of resultant polymer nanostructures via solution wetting. Also unclear is why solid nanorods generated by solution wetting can nearly replicate cylindrical nanopores and have the diameter in good agreement with that of the nanopores.[11,12]

Table 1. Types of Nanostructures Generated from Different Solvents and PS with Various Weight-Average Molecular Weights[a]

mol wt (g/mol)	THF	MEK	THF + DCM (1/9, v/v)	MEK + DCM (1/9, v/v)	DCM
5200	●	●	●	●	●
25 000	●	●	●	●	□
65 000	●	●	●	●	□
152 000	●	●	●	●	○
390 000	●	●	●	●	○
650 000	●	●	●	●	○

[a] The six PS samples used have a same polydispersity index of 1.06. Black dot (●), square (□), and circle (○) represent solid nanorods, void-containing nanorods, and nanotubes respectively. The results of DCM were from the report by Wendorff et al.[11]

In the case of wetting AAO membranes with polymer solutions, an important factor has been omitted until now, that is, the surface property of alumina nanopore wall. It is well-known that alumina surfaces possess both Brønsted and Lewis acidic sites,[13−15] which are responsible for the favorable adsorption of electron-pair donor (EPD) solvents[16−19] or prototypical basic polymers.[20−23]When alumina is brought in contact with a polymer solution, different interfacial interactions can occur depending on the characteristics of polymer and solvent. However, to our knowledge, no report has highlighted the role of interfacial interactions in the control over the formation of polymer nanostructures by solution wetting. In this

* To whom correspondence should be addressed. Telephone: 86-10-62515757. Fax: 86-10-62516464. E-mail: jinzx@ruc.edu.cn.

10.1021/ma8024283 CCC: $40.75
Published on Web 01/12/2009

Scheme 1. Schematics of (a) an Alumina Surface with Hydroxyl Groups and (b) a Depletion Layer Formed in the Vicinity of an AAO Nanopore Wall

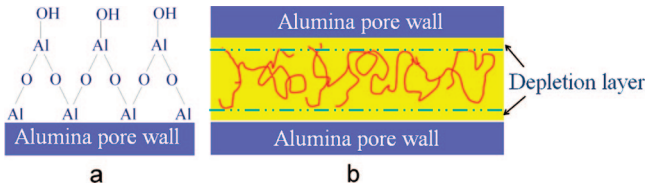

study, we focused on the wetting of AAO membranes with polymer solutions, using polystyrene (PS) as a model system. First, we aimed to find out how different interfacial affinity of polymer and solvent to alumina would influence the nanostructure morphologies. Our second purpose was to make it clear why solvent evaporation could enrich polymer inside nanopores and yield solid nanorods without a great amount of shrinkage compared with the pore size. Finally, we expected that besides 1D nanostructures other useful nanostructures such as nanospheres and nanocapsules could also be generated from the evaporation of polymer solutions inside AAO nanopores.

In a typical experiment of solution wetting, an AAO membrane (Whatman Anodisc 13, 0.2 μm; see Figure S1) was immersed in a PS solution for 24 h. Subsequently, the membrane was picked up from the solution and dried at ambient conditions. The membrane was finally etched by a 5 wt% NaOH solution to release the nanostructures for the characterization by scanning electron microscopy (SEM) and transmission electron microscopy (TEM). The detailed procedures can be found in the Supporting Information.

First, to evaluate the influence of interfacial interactions on the formation of polymer nanostructures, two EPD solvents, i.e., tetrahydrofuran (THF) and methyl ethyl ketone (MEK), were particularly chosen, owing to their strongly adsorbent nature toward alumina.[18,19] Additionally, to compare the results with those by Wendorff et al.[11] (in their study dichloromethane (DCM) was used as solvent), THF or MEK was added to DCM to prepare two cosolvents, with a small volume fraction (10%) of THF or MEK respectively. The concentrations of all PS solutions were fixed to 100 mg/mL. Here, concerning the effect of molecular weight, six nearly monodisperse PS with weight-average molecular weights ranging from 5 200 to 650 000 g/mol were tested (see Table 1). Table 1 summarizes the results obtained from the SEM and TEM characterization together with those by Wendorff et al. for comparison. According to their prediction, three modes of nanostructures, i.e., solid rods, void-containing rods and tubes, should occur in the specific ranges of molecular weight.[11] However, we found that the use of THF and MEK as solvents resulted in one mode of nanostructures: solid nanorods, showing no correlation to the molecular weights (Figure S3). Furthermore, because of the addition of THF or MEK to DCM, the previously reported morphologies of nanotubes and void-containing nanorods from high and intermediate molecular weight polymers changed dramatically to solid nanorods.

Obviously, the predominant factor in the control over the nanorod formation here is not molecular weight but interfacial interaction. It has been known that alumina surfaces exposed to ambient environment terminate in an outermost layer of hydroxyl groups (Scheme 1a), which contribute to the strong interfacial interactions between alumina and EPD solvents.[13−19] However, PS-alumina interactions have been proven unfavorable.[23,24] When an AAO nanopore is filled with a PS/THF or PS/MEK solution, one would reasonably expect that the acidic pore wall prefers the solvent to PS and the polymer chains avoid the vicinity of the alumina surface, leading to the formation of a depletion layer[25,26] initially (Scheme 1b). Thus, as the solvent evaporates, PS concentrates at the center of the nanopore and a nanorod consequently forms. This interpretation is also supported by the formation of nanorods from those two cosolvents.

Considering that the volume fraction of solvent was rather larger than that of polymer, a great amount of shrinkage should be expected in the obtained nanorods after solvent evaporation. However, when compared with the pore size, the actual shrinkage observed was quite small in the nanorods (Figure S4). The solid nanorods could nearly replicate the cylindrical nanopores. This phenomenon has been previously reported in the literature.[11,12] To find out how solvent evaporation could enrich polymer in cylindrical nanopores during the formation of nanorods, we performed the wetting of AAO membranes with PS/THF solutions with different concentrations (i.e., 10, 20, 32, 40, 100, and 150 mg/mL). The weight-average molecular weight of PS was fixed to 152 000 g/mol. The wetting procedures were modified: when picked up from the solution and before evaporation took place, the AAO membrane was rapidly dipped into pure THF to wash away the redundant solution outside the nanopores (see also route b in Figure S2). Note that the washing step was necessary for it could eliminate the influence of the polymer solution on the membrane surface, as discussed later.

Parts a and b of Figure 1 display the nanospheres generated from the wetting with a 20 mg/mL PS/THF solution. Wetting AAO membranes with PS/THF solutions of relatively low concentrations was found to give rise to the formation of nanospheres (see also Figure S5). When the concentration was increased to an intermediate range (e.g., to 32 or 40 mg/mL), nanocapsules and short nanorods predominantly occurred (Figures 1c,d and S6). And further increasing the initial concentration led to the formation of nanorods with higher aspect ratio. Parts e−g of Figure 1 show the nanorods produced from a 150 mg/mL PS/THF solution. The average rod diameter was roughly the same as the pore size. By careful examination of the morphology of the nanorods, we observed the presence of hemispherical caps at both ends of the nanorods (Figure 1e−g). This observation indicates that the mechanism for the nanorod formation here differs distinctly from what Russell et al. have proposed,[10] considering the fact that a meniscus has been found at the end of the nanorods in their case.

We now discuss the possible mechanisms responsible for the evolution from nanospheres to nanorods inside cylindrical nanopores. In the study of phase separation of a polymer solution in a capillary tube, Tanaka has shown that if the minority phase is less wettable to the tube wall, at the beginning of the phase separation it appears as small droplets and then the droplets coarsen by Brownian coagulation.[27] Similarly, as the solvent evaporates, the polymer concentrates at the center of nanopores; subsequently, droplets spontaneously occur possibly because of phase separation triggered by the solvent evaporation or breakup of solution cylinders induced by Rayleigh instabilities.[28−30] Because of the strong spatial confinement from alumina wall, these droplets are driven to locate one-dimensionally along the cylindrical nanopores. As demonstrated by Tanaka, this effect increases the chance of collision between droplets.[27] Thus, the droplets can grow larger by coalescence between adjacent ones. However, the geometrical constraints of cylindrical pores strongly inhibit free domain motion,[31−33] and therefore droplet

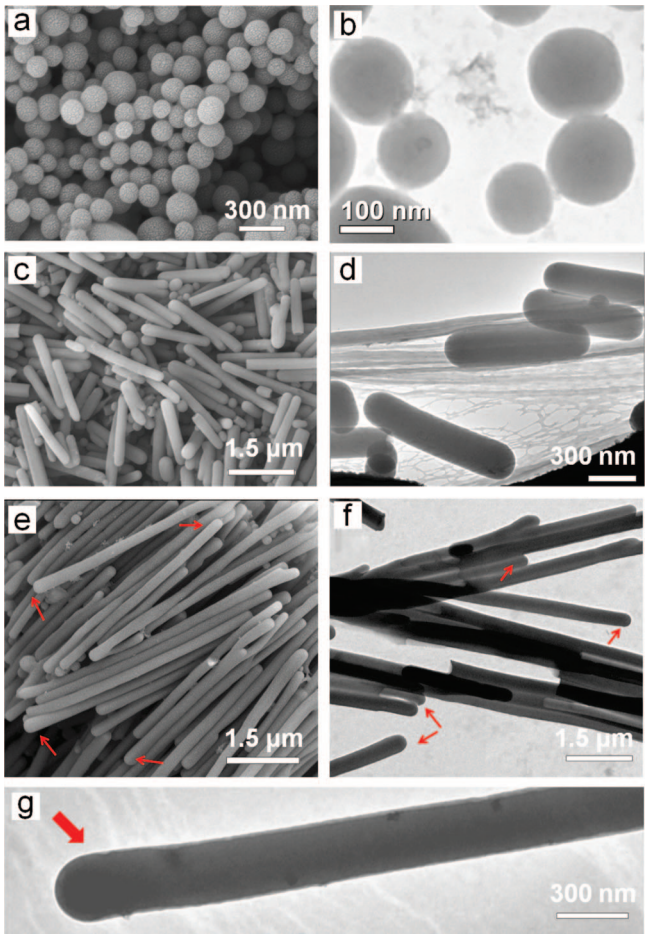

Figure 1. Micrographs of PS nanostructures resulting from PS/THF solutions with different initial concentrations: (a and b) for 20 mg/mL; (c and d) for 40 mg/mL; (e−g) for 150 mg/mL. Parts a, c, and e are SEM micrographs. Parts b, d, f, and g are TEM micrographs. The red arrows in parts e−g highlight the hemispherical caps at the ends of the nanorods.

coalescence can only occur between neighboring ones in a short-range manner.

If the initial concentration is rather low (e.g., 10 mg/mL) and the amount of polymer inside nanopores is small, considerable volume shrinkage should take place during the solvent evaporation process. Thus, after the complete evaporation of solvent, solidification of the droplets could produce relatively small polymer nanospheres with size below the pore diameter, as shown in Figure 2a. At a higher initial concentration, the amount of polymer should be larger, and therefore volume shrinkage resulting from the solvent evaporation is less remarkable. As the initial polymer concentration is increased (e.g., to 20 mg/mL), droplets can grow larger until having the comparable size as the pore diameter, as shown in Figure 2b. When the droplets approach the pore size, the confinement effects become extremely remarkable. By theoretical analysis and Monte Carlo simulation, Liu and co-workers have demonstrated that the pore confinement severely inhibits the mechanism of Ostwald ripening that a coarsening process commonly follows in bulk and predicted a "plug-tube-capsule" phase diagram.[31−33] Tanaka has observed through optical microscopy that the neighboring droplets merged and eventually transformed into capsules once their size exceeded the pore size.[27] Similarly in our case, the droplets can not grow spherically any more when encountering the extreme confinement from the nanopore wall. Instead, the mergence of droplets results in the formation of capsules

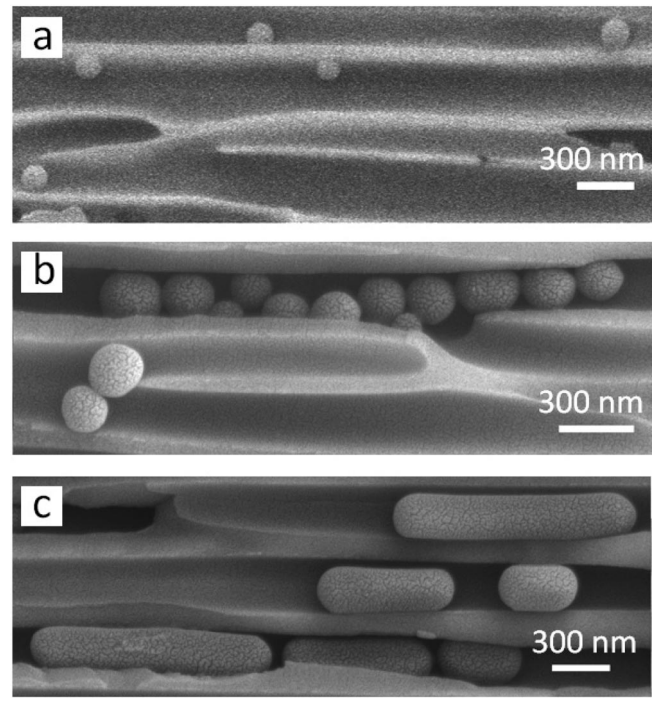

Figure 2. SEM micrographs of PS nanostructures embedded in the cleaved alumina nanopores. (a) Nanospheres from a 10 mg/mL PS/THF solution. (b) Nanospheres from a 20 mg/mL PS/THF solution. (c) Nanocapsules and nanorods from a 40 mg/mL PS/THF solution.

corresponding to the tubular constraints (Figure 2c). If the polymer concentration is rather high, the coalescence can occur between droplets, and droplets with capsules; in this manner, nanorods are formed. An important evidence for this interpretation for nanorod formation is the presence of hemispherical caps at both ends of the obtained nanorods.

Although increasing the polymer concentration could generate nanorods with higher aspect ratio, we found that the formation of long nanorods with length as the pore depth was not accessible if the polymer solution outside the nanopores was washed away. However, in a conventional process of wetting AAO with a polymer solution (without the washing step), long nanorods have commonly been obtained.[11,12] Moreover, if the washing step was not conducted, we found that nanospheres and nanocapsules could hardly be produced even at a low polymer concentration and the morphology mainly turned out to be solid nanorods. Thus, the diffusion of polymer from outside the nanopores is indeed present, and the outer solution acts as a reservoir which feeds polymer into the nanopores. Inside the nanopores the coarsening process of droplets on the one hand tends to form nanorods; on the other hand, the coarsening should be assisted by the polymer reservoir outside the nanopores. The coupling of these two processes may be responsible for the enrichment of polymer in the pore space.

In conclusion, for the wetting of AAO templates with polymer solutions, the importance of interfacial interactions in controlling the resultant polymer nanostructure morphologies has been revealed in this study. In particular, we have demonstrated that the nanorod morphology formed by solution wetting is strongly dependent upon the solvents used which have preferential affinity to alumina. More importantly, we have shown that the coarsening process from spheres to capsules to rods in cylindrical nanopores serves as the formation mechanism for nanorods. From a practical viewpoint, our observation provides a facile approach for fabricating polymer nanospheres and nanocapsules that can be directed by cylindrical nanopores into ordered arrays.

Furthermore, we report a unique kind of polymer nanostructures, i.e., hemispherically capped nanorods, which may have many potential applications such as sensitive chemical and biochemical sensors.

Acknowledgment. The authors gratefully acknowledge the National Nature Science Foundation of China (Grant 50503025) and Renmin University of China for financial support.

Supporting Information Available: Text giving detailed experimental procedures and supplementary figures showing SEM and TEM micrographs and scheme showing the wetting. This material is available free of charge via the Internet at http://pubs.acs.org.

References and Notes

(1) Martin, C. R. *Chem. Mater.* **1996**, *8*, 1739–1746.
(2) Ai, S.; Lu, G.; He, Q.; Li, J. *J. Am. Chem. Soc.* **2003**, *125*, 11140–11141.
(3) Steinhart, M.; Wendorff, J. H.; Greiner, A.; Wehrspohn, R. B.; Nielsch, K.; Schilling, J.; Choi, J.; Gösele, U. *Science* **2002**, *296*, 1997.
(4) Steinhart, M.; Wehrspohn, R. B.; Gösele, U.; Wendorff, J. H. *Angew. Chem., Int. Ed.* **2004**, *43*, 1334–1344.
(5) Moon, S. I.; McCarthy, T. J. *Macromolecules* **2003**, *36*, 4253–4255.
(6) Steinhart, M.; Senz, S.; Wehrspohn, R. B.; Gösele, U.; Wendorff, J. H. *Macromolecules* **2003**, *36*, 3646–3651.
(7) Chen, J. T.; Zhang, M. F.; Russell, T. P. *Nano Lett.* **2007**, *7*, 183–187.
(8) Luo, Y.; Lee, S. K.; Hofmeister, H.; Steinhart, M.; Gösele, U. *Nano Lett.* **2004**, *4*, 143–147.
(9) Wu, H.; Wang, W.; Yang, H.; Su, Z. *Macromolecules* **2007**, *40*, 4244–4249.
(10) Zhang, M. F.; Dobriyal, P.; Chen, J. T.; Russell, T. P.; Olmo, J.; Merry, A. *Nano Lett.* **2006**, *6*, 1075–1079.
(11) Schlitt, S.; Greiner, A.; Wendorff, J. H. *Macromolecules* **2008**, *41*, 3228–3234.
(12) O'Brien, G. A.; Quinn, A. J.; Tanner, D. A.; Redmond, G. *Adv. Mater.* **2006**, *18*, 2379–2383.
(13) Tsyganenko, A. A.; Mardilovich, P. P. *J. Chem. Soc., Faraday Trans.* **1996**, *92*, 4843–4852.
(14) Adiga, S. P.; Zapol, P.; Curtiss, L. A. *J. Phys. Chem. C* **2007**, *111*, 7422–7429.
(15) Ballinger, T. H.; Yates, J. T. *Langmuir* **1991**, *7*, 3041–3045.
(16) Reichardt, C. In *Solvents and Solvent Effects in Organic Chemistry*; Wiley-VCH: Weinheim, Germany, 2003.
(17) Khaleel, A. A.; Klabunde, K. J. *Chem. Eur. J.* **2002**, *8*, 3991–3998.
(18) Uguina, M. A.; Sotelo, J. L.; Delgado, J. A.; Gómez, J. M.; Celemín, L. I. *Sep. Purif. Technol.* **2005**, *42*, 91–99.
(19) Howard, K. E.; Lakeman, C. D. E.; Payne, D. A. *J. Am. Ceram. Soc.* **1990**, *73*, 2543–2546.
(20) Konstadinidis, K.; Thakkar, B.; Chakraborty, A.; Potts, L. W.; Tannenbaum, R.; Tirrell, M.; Evans, J. F. *Langmuir* **1992**, *8*, 1307–1317.
(21) McCafferty, E. *J. Electrochem. Soc.* **2003**, *150*, B342–B347.
(22) Tannenbaum, R.; King, S.; Lecy, J.; Tirrell, M.; Potts, L. *Langmuir* **2004**, *20*, 4507–4514.
(23) Prause, S.; Spange, S. *J. Phys. Chem. B* **2004**, *108*, 5734–5741.
(24) Rittigstein, P.; Torkelson, J. M. *J. Polym. Sci., Part B: Polym. Phys.* **2006**, *44*, 2935–2943.
(25) de Gennes, P. G. *Adv. Colloid Interface Sci.* **1987**, *27*, 189–209.
(26) Fondecave, R.; Brochard-Wyart, F. *Macromolecules* **1998**, *31*, 9305–9315.
(27) Tanaka, H. *Phys. Rev. Lett.* **1993**, *70*, 53–56.
(28) Rayleigh, L. *Proc. London Math. Soc.* **1878**, *10*, 4–13.
(29) de Gennes, P. G.; Brochard-Wyart, F.; Quere, D. *Capillarity and Wetting Phenomena*; Springer: New York, 2004.
(30) Qin, Y.; Lee, S. M.; Pan, A.; Gösele, U.; Knez, M. *Nano Lett.* **2008**, *8*, 114–118.
(31) Liu, A. J.; Durian, D. J.; Herbolzheimer, E.; Safran, S. A. *Phys. Rev. Lett.* **1990**, *65*, 1897–1900.
(32) Monette, L.; Liu, A. J.; Grest, G. S. *Phys. Rev. A* **1992**, *46*, 7664–7679.
(33) Liu, A. J.; Grest, G. S. *Phys. Rev. A* **1991**, *44*, R7894–R7897.

MA8024283